



High-content screening in zebrafish identifies perfluorooctanesulfonamide as a potent developmental toxicant[☆]

Subham Dasgupta ^a, Aalekhya Reddam ^{a, b}, Zekun Liu ^c, Jinyong Liu ^c, David C. Volz ^{a, *}

^a Department of Environmental Sciences, University of California, Riverside, CA, USA

^b Environmental Toxicology Graduate Program, University of California, Riverside, CA, USA

^c Department of Chemical and Environmental Engineering, University of California, Riverside, CA, USA

ARTICLE INFO

Article history:

Received 14 September 2019

Received in revised form

27 October 2019

Accepted 30 October 2019

Available online xxx

Keywords:

PFAS

Perfluorooctanesulfonamide

Embryonic development

Zebrafish

Hepatotoxicity

ABSTRACT

Per- and polyfluoroalkyl substances (PFASs) have been used for decades within industrial processes and consumer products, resulting in frequent detection within the environment. Using zebrafish embryos, we screened 38 PFASs for developmental toxicity and revealed that perfluorooctanesulfonamide (PFOSA) was the most potent developmental toxicant, resulting in elevated mortality and developmental abnormalities following exposure from 6 to 24 h post fertilization (hpf) and 6 to 72 hpf. PFOSA resulted in a concentration-dependent increase in mortality and abnormalities, with surviving embryos exhibiting a >12-h delay in development at 24 hpf. Exposures initiated at 0.75 hpf also resulted in a concentration-dependent delay in epiboly, although these effects were not driven by a specific sensitive window of development. We relied on mRNA-sequencing to identify the potential association of PFOSA-induced developmental delays with impacts on the embryonic transcriptome. Relative to stage-matched vehicle controls, these data revealed that pathways related to hepatotoxicity and lipid transport were disrupted in embryos exposed to PFOSA from 0.75 to 14 hpf and 0.75 to 24 hpf. Therefore, we measured liver area as well as neutral lipids in 128-hpf embryos exposed to vehicle (0.1% DMSO) or PFOSA from 0.75 to 24 hpf and clean water from 24 to 128 hpf, and showed that PFOSA exposure from 0.75 to 24 hpf resulted in a decrease in liver area and increase in yolk sac neutral lipids at 128 hpf. Overall, our findings show that early exposure to PFOSA adversely impacts embryogenesis, an effect that may lead to altered lipid transport and liver development.

© 2019 Elsevier Ltd. All rights reserved.

1. Introduction

Per- and polyfluoroalkyl substances (PFASs) have been widely used for decades within an array of industrial processes and consumer products such as Teflon coating in cooking utensils, fabrics, food packaging, fire-fighting foams, and mechanical lubrication (Stahl et al., 2011). While high thermal and chemical stability of PFASs are critical for enhanced efficacy, these physicochemical properties lead to environmental persistence, bioaccumulation, and the potential for toxicity. Indeed, discharge from fluorochemical industries and foam products have led to significant PFAS contamination within water bodies across the world. For example, Hu et al. found that levels of PFASs within drinking water

serving ~6 million residents across the United States exceeded the U.S. Environmental Protection Agency's regulatory threshold of 70 ng/L (~0.16 μM), raising concerns about potential health effects following long-term exposure (Hu et al., 2016). Human exposure to PFASs primarily occurs via contaminated seafood and drinking water as well as consumer products and contaminated indoor dust. Indeed, elevated (μg/L) levels of PFASs have been measured within human blood samples – including maternal blood and fetal cord blood within prenatal environments (Inoue et al., 2004; Monroy et al., 2008; Stahl et al., 2011) – raising concerns about the potential for *in utero* exposure and developmental toxicity.

Within the broader class of PFASs, perfluorooctanesulfonic acid (PFOS) and perfluorooctanoic acid (PFOA) are the most frequently detected PFASs within drinking water, food samples, human blood, and breast milk samples, with concentrations approaching up to ~12 μg/L in maternal and cord blood samples (Fei et al., 2007; Inoue et al., 2004; Monroy et al., 2008). Although evidence of developmental abnormalities following PFAS exposure is limited within

[☆] This paper has been recommended for acceptance by Dr. Sarah Harmon.

* Corresponding author. Department of Environmental Sciences, University of California, Riverside, CA, 92521, USA.

E-mail address: david.volz@ucr.edu (D.C. Volz).

rodent models, decreased birth weight, still births, and altered kidney and liver sizes within offspring have been observed in some studies (Stahl et al., 2011). However, several studies within zebrafish have shown that early developmental exposures of PFOS and perfluororonanoic acid (PFNA) alter the normal trajectory of development, including impacts on the swim bladder, spine, and pancreas as well as pathways related to thyroid hormone synthesis, estrogen synthesis and reactive oxygen species (Chen et al., 2014; Liu et al., 2015; Sant et al., 2017; Sant et al., 2018). In addition to PFOS, other PFAS sulfonates have also been associated with a diverse range of developmental effects in zebrafish. For example, potassium nonafluorobutanesulfonate (PFBS) exposure results in abnormal pancreatic development through disturbance of lipid homeostasis (Sant et al., 2019), whereas potassium perfluorohexane-1-sulfonate (PFHxS) and perfluorohexanoic acid (PFHxA) exposure induces developmental neurotoxicity and malformations within zebrafish (Annunziato et al., 2019). However, developmental toxicity data are limited or unavailable for a number of other PFASs in commerce, particularly for early developmental windows that include cell fate specification and dorsoventral patterning.

To increase our knowledge about the potential for PFAS-induced toxicity during early embryonic development, we relied on high-content screening to test the potential toxicity of 38 different PFASs within the first 72 h of zebrafish development, a window that includes gastrulation, somitogenesis, and organogenesis (Kimmel et al., 1995). Based on this screen, perfluorooctanesulfonamide (PFOSA) was identified as the most potent developmental toxicant relative to all PFASs evaluated. Therefore, we further investigated the mechanisms of PFOSA-induced developmental toxicity by relying on 1) phenotyping and whole-mount immunohistochemistry to quantify developmental deformities as well as impacts on epiboly – an early developmental process that is critical for determining cell fate during later stages of development; 2) mRNA-sequencing to quantify whole-transcriptome responses to PFOSA exposure within the first 24 h of development; and 3) based on our mRNA-sequencing data, morphological assessments and Oil Red O staining to quantify the potential for PFOSA-induced impacts on the liver after five days of development.

2. Materials and methods

2.1. Animals

Adult wildtype (5D) zebrafish were maintained and bred on a recirculating system using previously described procedures (Mitchell et al., 2018). Adult breeders were handled and treated in accordance with Institutional Animal Care and Use Committee-approved animal use protocol (#20180063) at the University of California, Riverside.

2.2. Chemicals

Table S1 includes a list of all 38 PFASs screened as well as the source (vendor), lot number, catalog number, and percent purity for each PFAS. Stock solutions were prepared by dissolving chemicals in either high-performance liquid chromatography-grade dimethyl sulfoxide (DMSO) or a sodium hydroxide (NaOH) solution (20 or 40 mM NaOH prepared in deionized water), resulting in stock concentrations of 50 mM or 10 mM PFAS, respectively; NaOH was used as a solvent for a subset of PFAS acids to reduce volatilization from DMSO-based stocks. All stock solutions were stored in 5-ml glass vials at room temperature. All working solutions (50 μ M PFAS) were freshly prepared by spiking stock solutions into water derived from our recirculating system (pH and conductivity of

~7–8 and ~950 μ S, respectively), resulting in a final DMSO concentration of 0.1% or NaOH concentration of 0.1 or 0.2 mM for 20 and 40 mM NaOH stocks, respectively. Stock concentrations as well as DMSO and NaOH concentrations within all stock and working solutions for each PFAS are also included within **Table S1**. For all experiments, embryos were incubated under static conditions at 28 °C under a 14-h:10-h light:dark cycle for the entire duration of exposure.

2.3. High-content screening of PFASs

To screen 38 PFASs for developmental toxicity, we used black 384-well microplates with 0.17-mm glass-bottom wells (Matrical Bioscience, Spokane, Washington). Newly fertilized eggs were collected immediately after spawning and incubated in petri dishes until 5 hpf. Between 5 and 6 hpf, dead embryos were discarded, and live and normal embryos (~30–50% epiboly) were isolated and transferred to 384-well plates, resulting in one embryo per well and eight embryos per treatment group. Each well contained 50 μ l of either vehicle (0.1% DMSO, 0.1 mM NaOH, or 0.2 mM NaOH depending on the PFAS stock) or treatment solution at a concentration of 50 μ M PFAS. The plate was then covered with a lid, wrapped in parafilm, and incubated under static conditions at 28 °C under a 14-h:10-h light:dark cycle. At 24 and 72 hpf, all plates were removed from the 28 °C incubator, incubated at 4 °C for ~20 min to anesthetize the embryos, and imaged on our ImageXpress Micro XLS Widefield High-Content Screening System (Molecular Devices, Sunnyvale, California) using previously described automated acquisition protocols within MetaXpress 6.0.3.1658 (Molecular Devices) (Vliet et al., 2017). After image acquisition, each embryo was recorded as normal, abnormal relative to time-matched controls (including embryos with delayed development), or dead (coagulated embryos or developed embryos lacking a heartbeat). Based on these criteria, percent survival and percent normal for each treatment group were calculated.

2.4. PFOSA concentration-response experiments

Following our initial screen, survival and developmental deformities within PFOSA treatments were assessed in concentration-response format using clean, 50-mm glass petri dishes. For each exposure scenario described below, embryos (30 per petri dish) were exposed to 10 ml of vehicle (0.1% DMSO) or PFOSA (6.25, 12.5, 25 and 50 μ M) within three replicate petri dishes per treatment concentration. Newly fertilized eggs were collected immediately after spawning and sorted into 2- to 4-cell-stage embryos (Kimmel et al., 1995). Exposures were initiated at either 0.75 hpf (4-cell stage), 6 hpf (~50% epiboly), or 12 hpf (segmentation), and embryos were incubated under static conditions at 28 °C under a 14-h:10-h light:dark cycle. At 24 hpf, embryos were incubated at 4 °C for ~20 min (for anesthesia) and then imaged using a Leica MZ10 F stereomicroscope equipped with a DMC2900 camera. Following imaging, each live embryo was grouped into one of four different developmental windows (>21 somites; >10 somites to 21 somites; bud to 10 somites; or within or earlier than epiboly). Percent survival as well as percent of live embryos within each developmental window were quantified by replicate petri dish.

2.5. Cell height measurements for epiboly assessment

Using previously described protocols (Kupsco et al., 2017; Vliet et al., 2018), cell height was used to quantify the magnitude of PFOSA-induced epiboly delays. Embryos (30 per 50-mm glass petri dish) were exposed from 0.75 to 6 hpf to 10 ml of vehicle (0.1% DMSO) or PFOSA (6.25, 12.5, 25, or 50 μ M) within three replicate

petri dishes per treatment concentration. At 6 hpf, 10 randomly selected live embryos per petri dish were imaged using a Leica MZ10 F stereomicroscope equipped with a DMC2900 camera. All cell height measurements were performed using ImageJ.

2.6. Cytoskeletal staining

To assess the impacts of PFOSA on blastomeric cell area, embryos (30 per 50-mm glass petri dish) were exposed to vehicle (0.1% DMSO) or 25 μ M PFOSA (three replicate petri dishes per treatment) from 0.75 hpf to 3 or 5 hpf and then fixed in 4% paraformaldehyde/1X phosphate-buffered saline (PBS). Fixed embryos were then dechorionated and stained with 1:200 AlexaFluor 488-conjugated phalloidin (Millipore Sigma) using previously described protocols (Dasgupta et al., 2019). Embryos were then imaged using a Leica MZ10 F stereomicroscope equipped with a DMC2900 camera and GFP filter, and cell area was quantified using previously described protocols (Dasgupta et al., 2019).

2.7. Recovery experiments

To determine whether embryos recovered following early, transient exposure to PFOSA, embryos (30 per 50-mm glass petri dish) were treated with vehicle (0.1% DMSO) or 12.5 μ M PFOSA from 0.75 to 6 hpf (six replicate petri dishes per treatment). At 6 hpf, embryos from three replicate dishes were transferred to freshly prepared vehicle (0.1% DMSO) solution, while embryos from the remaining three replicate dishes were transferred to freshly prepared treatment (12.5 μ M PFOSA) solution. Embryos were then incubated at 28 °C under a 14-h:10-h light:dark cycle from 6 to 24 hpf. At 24 hpf, embryos were imaged and assessed as described in Section 2.4.

2.8. mRNA-sequencing

To assess the potential association of developmental delays with impacts on the transcriptome, embryos (30 per 50-mm glass petri dish) were exposed to vehicle (0.1% DMSO) or 12.5 μ M PFOSA from 0.75 hpf to 14 or 24 hpf (eight replicate petri dishes per treatment) and incubated at 28 °C under a 14-h:10-h light:dark cycle. At 24 hpf, 60 embryos were pooled from two replicate petri dishes, snap frozen in liquid nitrogen, and stored at -80 °C, resulting in four replicate embryo pools per treatment and time-point. Embryos were homogenized in 2-ml cryovials using a PowerGen Homogenizer (Thermo Fisher Scientific, Waltham, MA, USA), resulting in a total of 16 samples. Following homogenization, an SV Total RNA Isolation System (Promega, Madison, WI, USA) was used to extract total RNA from each replicate sample following the manufacturer's instructions. RNA quantity and quality were confirmed using a Qubit 4.0 Fluorometer (Thermo Fisher Scientific, Waltham, MA, USA) and 2100 Bioanalyzer system (Agilent, Santa Clara, CA, USA), respectively. Based on sample-specific Bioanalyzer traces, the RNA Integrity Number (RIN) was >8 for all RNA samples used for library preparations. Libraries were prepared using a QuantSeq 3' mRNA-Seq Library Prep Kit FWD (Lexogen, Vienna, Austria) and indexed by treatment replicate following the manufacturer's instructions. Library quantity and quality were confirmed using a Qubit 4.0 Fluorometer and 2100 Bioanalyzer system, respectively. Libraries were then pooled, diluted to a concentration of 1.3 pM (with 1% PhiX control) and single read (1X75) sequenced on our Illumina Miniseq Sequencing system (San Diego, California, USA) using a 75 cycle High-Output Reagent Kit.

All sequencing data were uploaded to Illumina's BaseSpace in real-time for downstream analysis of quality control. Raw Illumina (fastq.gz) sequencing files (16 files) are available via NCBI's

BioProject database under BioProject ID PRJNA563973, and a summary of sequencing run metrics are provided in Table S11 (>87.41% of reads were \geq Q30). All 16 raw and indexed Illumina (fastq.gz) sequencing files were downloaded from BaseSpace and uploaded to Bluebee's genomics analysis platform to align reads against zebrafish genome assembly GRCz10. After combining treatment replicate files, a DESeq2 application within Bluebee (Lexogen Quantseq DE 1.3) was used to identify significant treatment-related effects on transcript abundance. Differentially expressed genes based on treatment-specific comparisons ($p_{adj} < 0.05$) were imported into Qiagen's Ingenuity Pathway Analysis (Germantown, MD, USA), as well as DAVID Bioinformatic Resources 6.8. Within IPA, a Tox Analysis was performed based on a q-threshold of 0.05 (Reddam et al., 2019), and further downstream assessments were performed based on the most significantly affected categories identified within the Canonical Pathways and Tox Lists. Within DAVID, a Gene Ontology analysis was performed and results from GOTERM_MF_DIRECT (representing molecular functions) were used.

2.9. Liver area measurements and Oil Red O (ORO) staining

Quantitative assessments of liver area and body length were performed using previously described protocols (Reddam et al., 2019). Briefly, embryos (30 per 50-mm glass petri dish) were exposed to vehicle (0.1% DMSO) or 0.78 μ M PFOSA from 0.75 to 24 hpf (three replicate dishes per treatment) and then transferred to clean water until 128 hpf; the concentration of PFOSA was selected based on an initial concentration-response experiment. At 128 hpf, surviving embryos were euthanized by incubating at 4 °C for 1 h followed by fixation in 4% paraformaldehyde/1X PBS. Fixed embryos were then imaged for body length and liver area using a Leica MZ10 F stereomicroscope equipped with a DMC2900 camera.

Following imaging for liver assessments, fixed 128-hpf embryos exposed to vehicle (0.1% DMSO) and 0.78 μ M PFOSA solutions were stained with ORO to quantify neutral lipids using previously described protocols (Reddam et al., 2019). ORO-stained embryos were then imaged using a Leica MZ10 F stereomicroscope equipped with a DMC2900 camera. Images were color-inverted and staining intensity within the yolk sac, trunk and head were quantified using the "Mean gray intensity" function within ImageJ.

2.10. Statistics

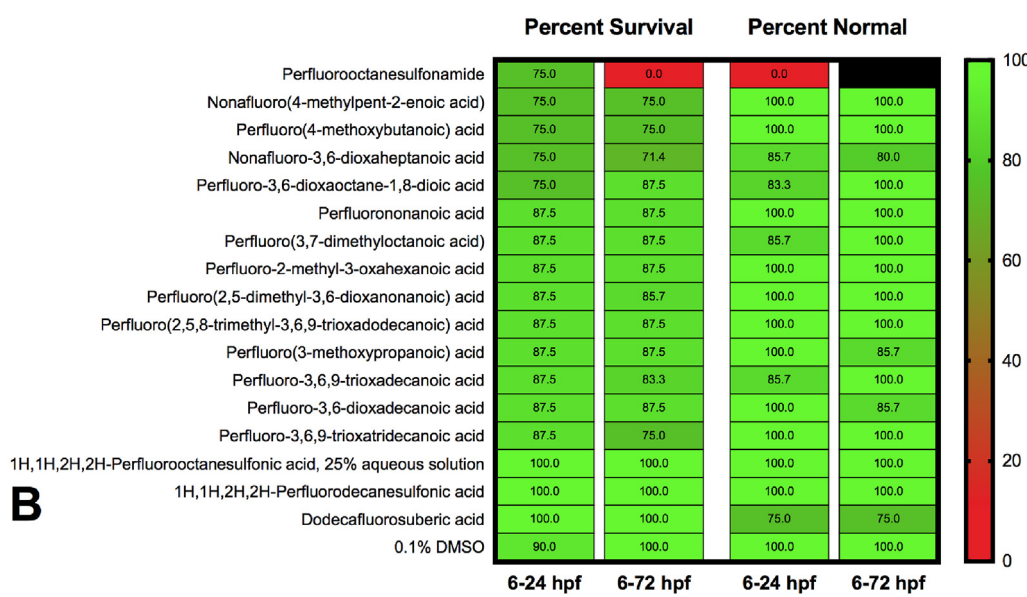
All phenotypic, morphometric, and immunofluorescence data were log-transformed and statistical differences in effects were estimated using either a two-tailed *t*-test or one-way ANOVA followed by a Dunnett's post-hoc test ($p < 0.05$). For all phenotypic assessments at 24 hpf, statistical analyses were based on the percent of normal (>21 somite stage) embryos at 24 hpf. For sequencing, statistical analyses were performed within the Bluebee platform using the Lexogen Quantseq DE 1.3 pipeline ($p_{adj} < 0.05$).

3. Results

3.1. PFOSA induces a concentration-dependent decrease in survival and delay in embryonic development by 24 hpf

Among the 38 PFASs tested, PFOSA was the only PFAS that induced embryonic toxicity following exposure to a limit concentration (50 μ M) from 6 to 72 hpf. At 24 hpf, 100% of PFOSA-exposed embryos were abnormal and/or delayed in development, and no PFOSA-exposed embryos survived by 72 hpf (Fig. 1A). The remaining 37 PFASs (including PFOS and PFOA) did not adversely impact survival nor development following exposure to a limit

A

DMSO-dissolved stocks

B

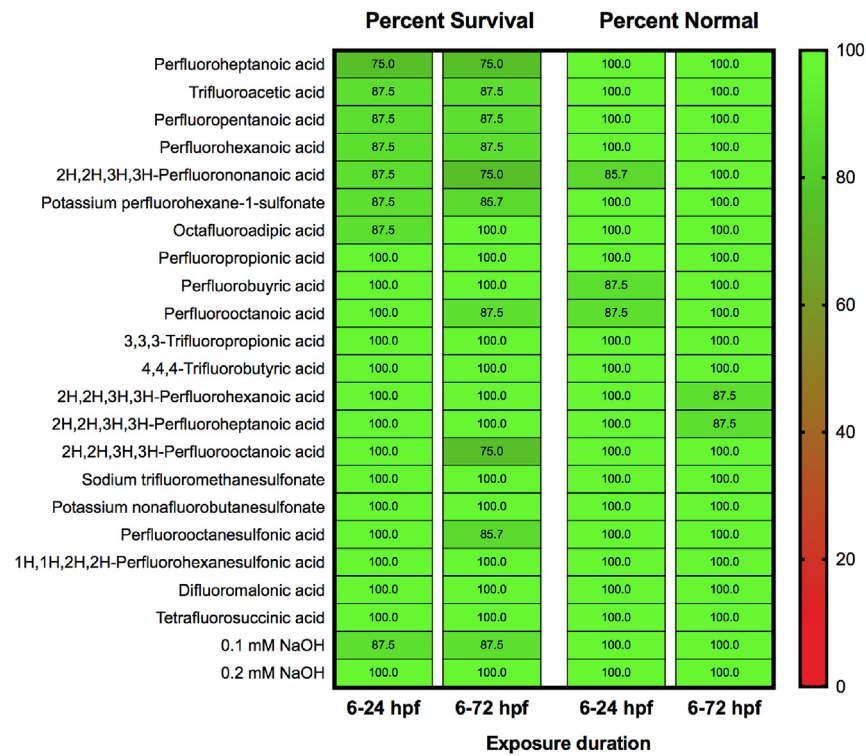
NaOH-dissolved stocks

Fig. 1. High-content screening of 38 PFASs (at 50 μ M) within zebrafish identifies PFOSA as a developmental toxicant. Numbers within the heatmaps represent percent survival and percent normal embryos; all exposures were initiated at 6 hpf. Each treatment consisted of eight replicate embryos (one embryo per well) within a 384-well plate. Compound stocks within (A) and (B) were prepared in 100% DMSO and NaOH (0.1 or 0.2 mM), respectively.

concentration (50 μ M) from 6 to 72 hpf (Fig. 1A and B). PFOSA exposure from 0.75 to 24 hpf and 6–24 hpf resulted in a concentration- and exposure duration-dependent decrease in survival by 24 hpf (Fig. 2A), where longer exposure durations resulted in a decrease in the lowest observed effect concentrations based on survival (50 μ M and 25 μ M PFOSA for exposures from 6 to 24 hpf and 0.75–24 hpf, respectively). Similarly, PFOSA-induced abnormalities and developmental delays within surviving embryos were dependent on concentration and exposure duration, where longer

exposure durations resulted in a decrease in the lowest observed effect concentrations based on developmental delays (25 μ M, 12.5 μ M, and 6.25 μ M for exposures from 0.75 to 24 hpf, 6–24 hpf, and 12–24 hpf, respectively) (Fig. 2B, C, and 2D).

3.2. Initiation of PFOSA exposure at 0.75 hpf leads to epiboly delays at 6 hpf

Using cell height as a readout, exposure to PFOSA from 0.75 to 6

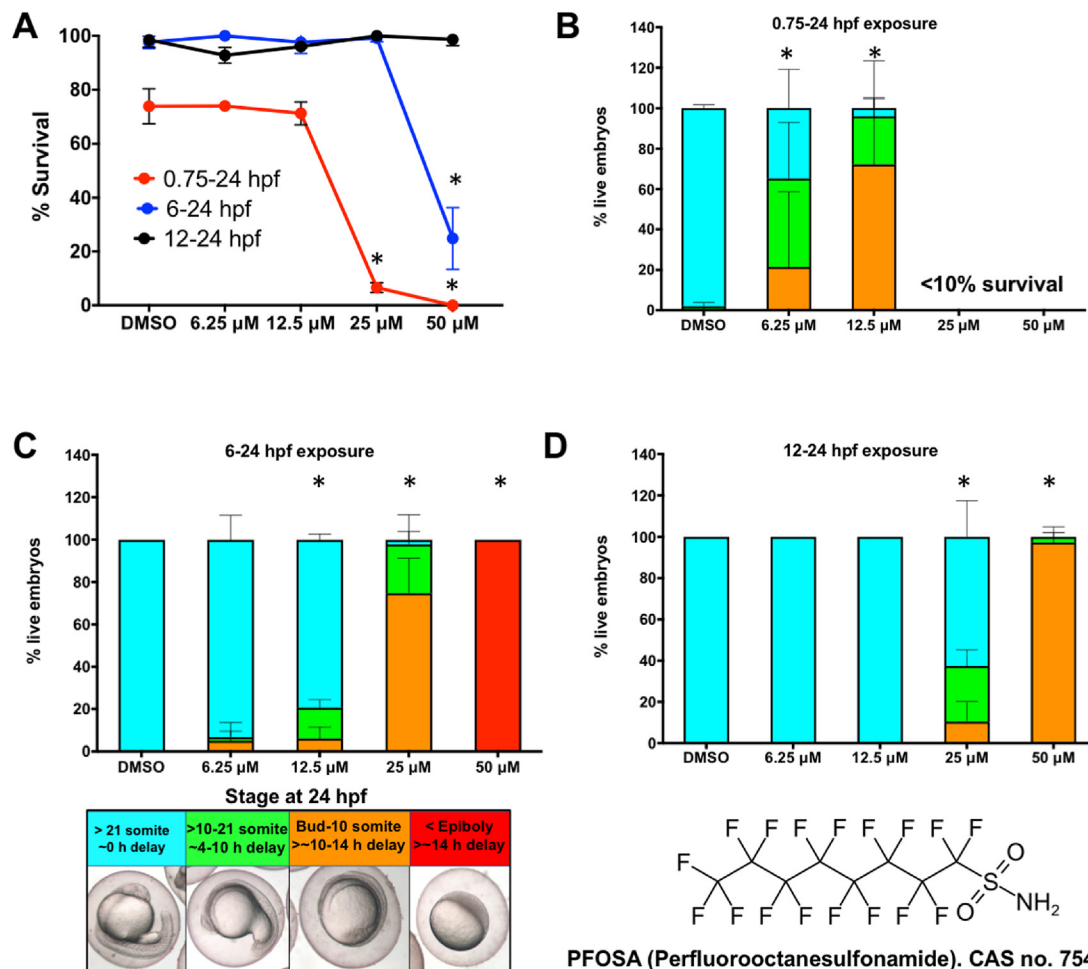


Fig. 2. PFOSA exposure results in a concentration-dependent decrease in survival (A) and increase in developmental delays (B–D) at 24 hpf. Bars with different colors represent a range of developmental stages at 24 hpf. Each treatment includes three replicate dishes with 30 embryos per dish. Asterisk (*) denotes a significant difference ($p < 0.05$) in percent survival (A) or percentage of embryos at >21 somite stage (B–D) relative to vehicle (0.1% DMSO) controls within the same exposure period. The chemical structure and CAS No. of PFOSA are provided on the bottom right. (For interpretation of the references to color in this figure legend, the reader is referred to the Web version of this article.)

hpf resulted in a concentration-dependent delay in epiboly at 6 hpf (Fig. 3A). However, epiboly delays induced by 25 μM PFOSA were significantly less severe when exposure was initiated at 4 and 5 hpf, suggesting that PFOSA-induced epiboly defects were stronger when exposures were initiated within the first 3 h of development (Fig. 3B). Phalloidin-based immunostaining of the blastomeric area revealed that developmental delays were initiated between 3 and 5 hpf, as PFOSA exposures initiated at 0.75 hpf resulted in larger blastomeric cell area at 5 hpf but not 3 hpf (Fig. 3C and D). Phalloidin-based immunostaining also showed that initiation of PFOSA exposure at 0.75 hpf resulted in decreased levels of yolk sac-localized actin (Fig. 3E and S1), an outcome that phenocopied the effects of niclosamide within one of our prior studies (Vliet et al., 2019).

3.3. Embryos exposed to PFOSA from 0.75 to 6 hpf recover by 24 hpf

We assessed whether developmental delays at 24 hpf persisted following termination of PFOSA exposure at 6 hpf. In contrast to continuous PFOSA exposure from 0.75 to 24 hpf (Figs. 2B and 4), embryos exposed from 0.75 to 6 hpf, and then transferred to vehicle (0.1% DMSO) from 6 to 24 hpf, were morphologically identical to vehicle-treated embryos (Fig. 4), showing that transient exposure within the first 6 h of development did not lead to morphological

effects at 24 hpf.

3.4. mRNA-sequencing reveals that PFOSA disrupts hepatotoxicity-related pathways within the first 24 h of development

To assess PFOSA-induced impacts on the embryonic transcriptome, the abundance of transcripts were compared between two sets of treatments: 1) PFOSA (0.75–14 hpf) vs. DMSO (0.75–14 hpf) (Fig. 5A, C, and 5E) and 2) PFOSA (0.75–24 hpf) vs. DMSO (0.75–14 hpf) (Fig. 5B, D, and 5F). To preclude any artifacts due to stage-specific differences in development, the 0.75–14 hpf DMSO treatment was chosen as a reference group for both PFOSA exposure scenarios since PFOSA-exposed embryos at 14 and 24 hpf closely phenocopied DMSO-exposed embryos at 14 hpf (Fig. 5A and B, and S2). Tables S2–S11 contain sequencing metrics, DESeq2 output, DAVID output, and IPA output.

Based on these data, there was an increase in the abundance of significantly affected transcripts in PFOSA-exposed embryos at 24 hpf relative to 14 hpf even though embryos within both stages were phenotypically similar to each other as well as similar to DMSO-treated embryos at 14 hpf (Fig. 5A and B). IPA-based pathway analysis across all comparisons revealed that hepatotoxicity-related pathways were strongly affected relative to impacts on renal toxicity- and cardiotoxicity-related pathways (Fig. 5C and D;

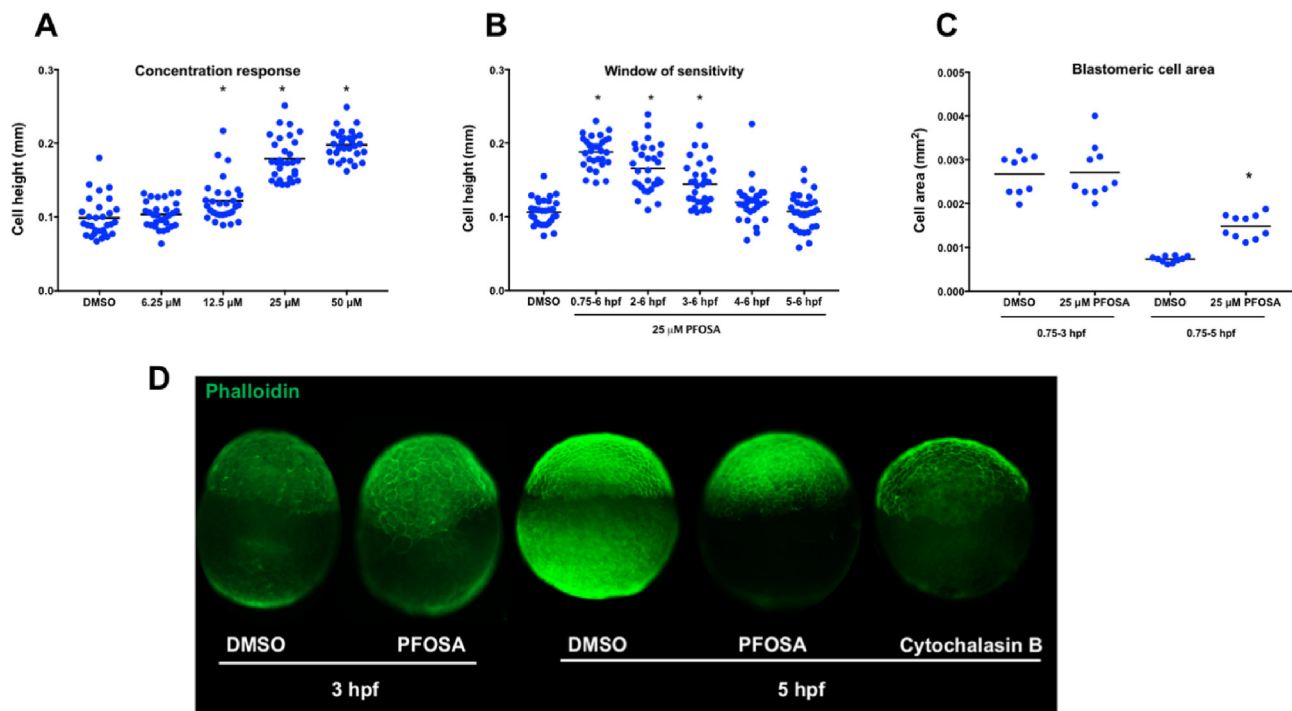


Fig. 3. Initiation of PFOSA exposure at 0.75 hpf induces a concentration-dependent increase in cell height at 6 hpf and corresponding delays in epiboly (A). A decrease in PFOSA exposure duration results in a decrease in the severity of epiboly delays (B). Data were derived from 30 embryos obtained from three replicate dishes per treatment. PFOSA exposures initiated at 0.75 hpf resulted in an increase in blastomeric cell area at 5 hpf – but not 3 hpf – based on cytoskeletal (phalloidin-based) immunostaining (C). Data from 10 embryos obtained from three replicate dishes per treatment. Representative images from phalloidin-stained embryos at 3 and 5 hpf (D); Cytochalasin B was used as a positive control. Asterisk (*) denotes a significant difference ($p < 0.05$) relative to vehicle (0.1% DMSO) controls.

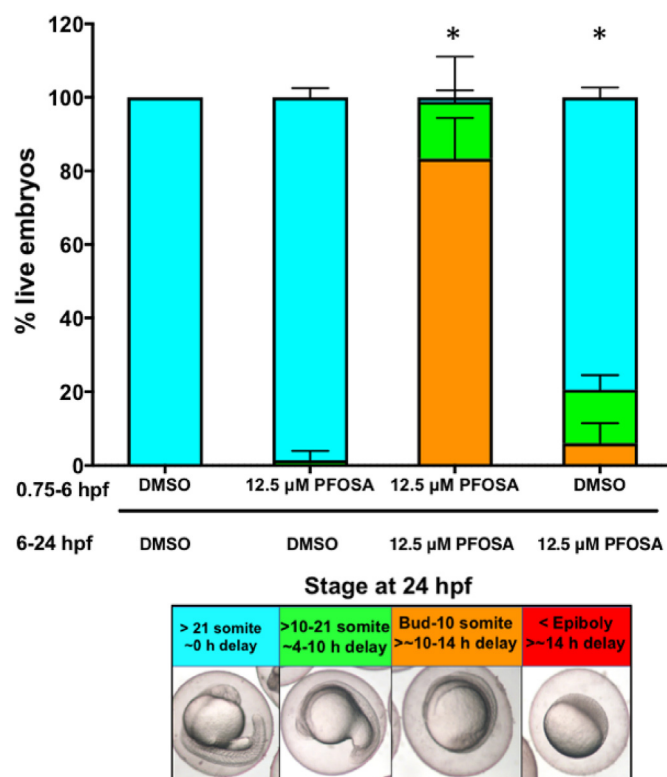


Fig. 4. PFOSA-induced developmental delays at 24 hpf are alleviated when exposures are terminated at 6 hpf. Data were derived from 30 embryos obtained from three replicate dishes per treatment. Asterisk (*) denotes a significant difference ($p < 0.05$) relative to vehicle (0.1% DMSO) controls.

Tables S9 and S10), an effect that increased in statistical significance from 14 to 24 hpf (Fig. 5E and F). Finally, DAVID-based molecular functions (Table S5) as well as IPA-based canonical pathways (Table S6) identified lipid binding and transport pathways as well as liver X receptor (LXR)/retinoid X receptor (RXR) pathways as strongly affected.

3.5. PFOSA exposure from 0.75 to 24 hpf results in decreased liver area and increased yolk sac-localized neutral lipids at 128 hpf

Based on results from IPA-based analysis within PFOSA-exposed embryos at 14 and 24 hpf, we investigated whether exposure to 0.78 μ M PFOSA from 0.75 to 24 hpf resulted in effects on liver morphology and neutral lipids at 128 hpf; 0.78 μ M PFOSA was chosen as a maximum tolerated concentration at 128 hpf (based on survival and gross morphology) following exposure from 0.75 to 24 hpf (Fig. 6A and G). To estimate impacts on liver development, we normalized liver area to body length in order to account for any effects due to developmental delays. PFOSA exposure from 0.75 to 24 hpf resulted in decreased liver area-to-body length ratio at 128 hpf (Fig. 6B and H) – an effect that occurred in the absence of significant effects on yolk sac area (Fig. 6C). Interestingly, ORO staining demonstrated that neutral lipids were significantly increased within the yolk sac of PFOSA-exposed embryos at 128 hpf (Fig. 6D); however, neutral lipids were not affected within the head or trunk (Fig. 6E and F).

4. Discussion

PFOSA is a sulfonamide used as a grease and water repellent for food packaging and, as a result, has been detected in packaged food (Perez et al., 2014; Tittlemier et al., 2006). Due to environmental

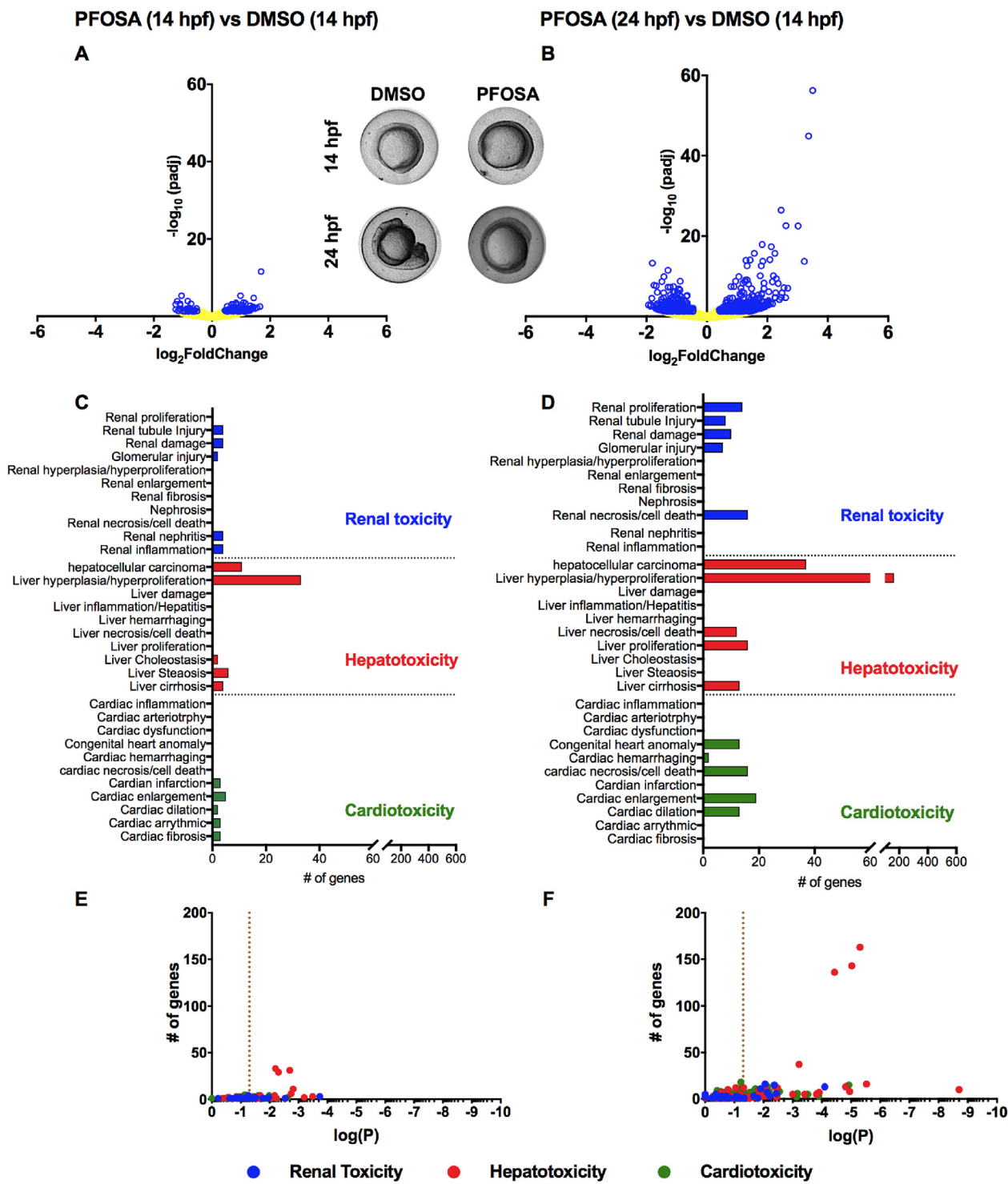


Fig. 5. Volcano plots representing differentially expressed genes based on mRNA-sequencing of embryos exposed to vehicle (0.1% DMSO) or 12.5 μ M PFOSA from 0.75 to 14 hpf and 0.75–24 hpf, followed by differential gene expression analysis between pairs of treatments within Bluebee's DESeq 1.3 pipeline (A–B). Blue dots represent transcripts with $p_{adj} < 0.05$. Inset shows representative images from 14 to 24 hpf embryos. Transcripts associated with cardiotoxicity, hepatotoxicity and renal toxicity as revealed by IPA-based Tox Analysis of differentially altered transcripts with $p_{adj} < 0.05$ (C–D). Scatterplots representing $\log(P)$ values relative to the number of genes for altered pathways related to cardiotoxicity, hepatotoxicity and renal toxicity (E–F). Vertical dashed line represents a p -value = 0.05. (For interpretation of the references to color in this figure legend, the reader is referred to the Web version of this article.)

contamination of PFASs, measurable levels of PFOSA have also been detected in seafood (Fair et al., 2019). Within biological systems, PFOSA is an active de-coupler of oxidative phosphorylation (Starkov and Wallace, 2002) and can be metabolized into PFOS

(Olsen et al., 2005). PFOSA and its precursor – 2-(N-Methyl-perfluoroctane sulfonamido) acetic acid (Me-PFOSA-AcOH) – have been frequently detected within human serum samples (Calafat et al., 2006; Whitworth et al., 2016), including serum samples of

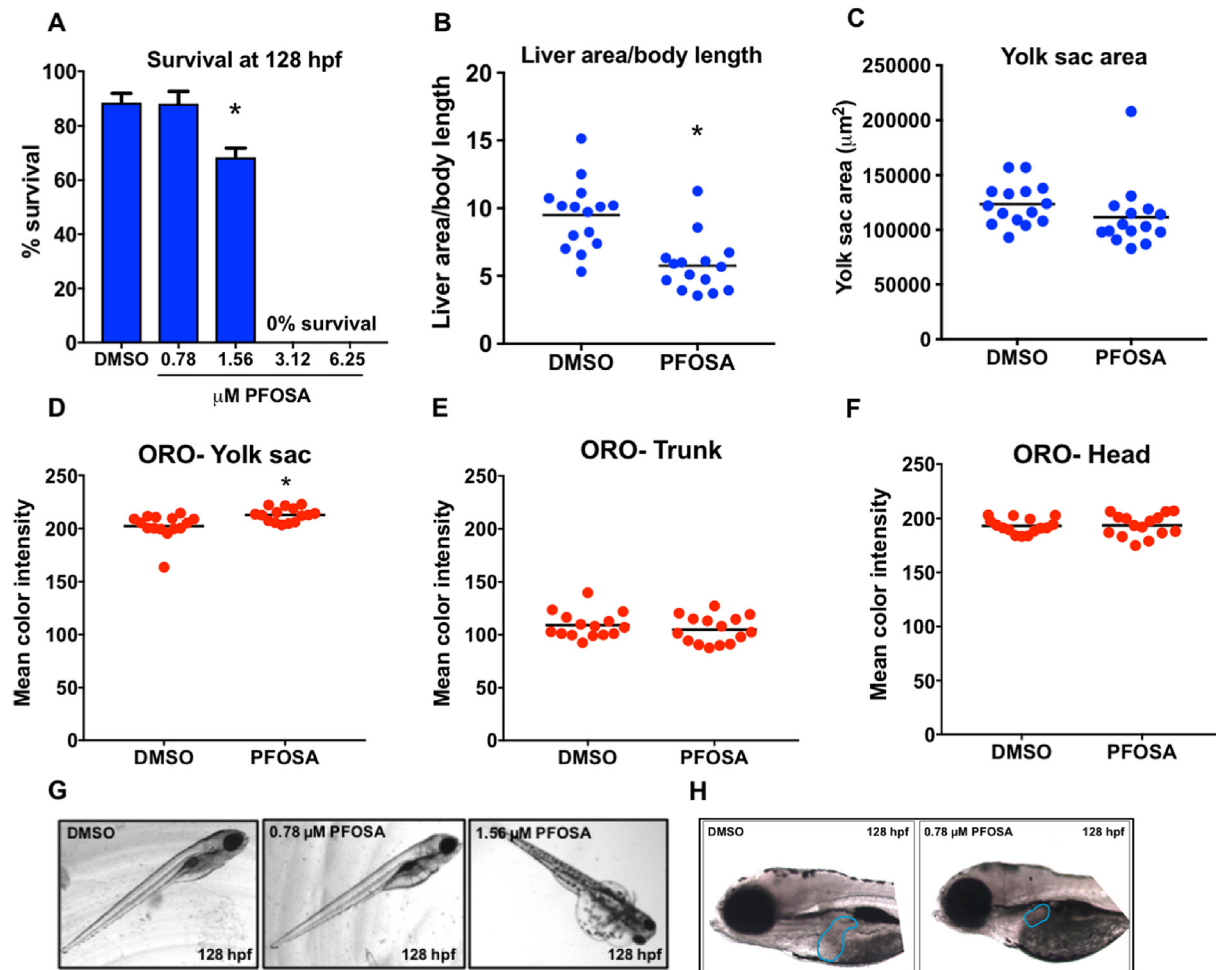


Fig. 6. Concentration-dependent decrease in survival of embryos exposed to PFOSA from 0.75 to 24 hpf, followed by incubation in clean water until 128 hpf (Fig. 6A). Data were derived from 30 embryos per replicate and three replicate dishes per treatment. Liver area normalized to body length (B), yolk sac area (C), and ORO staining within the yolk sac (D), trunk (E), and head (F) of embryos exposed to vehicle (0.1% DMSO) or 0.78 µM PFOSA from 0.75 to 24 hpf, followed by incubation in clean water until 128 hpf. Data were derived from five embryos per replicate and three replicate dishes per treatment. Asterisk (*) denotes significant difference ($p < 0.05$) relative to time-matched vehicle controls. Representative images from embryos exposed to PFOSA from 0.75 to 24 hpf, followed by incubation in clean water until 128 hpf (G, H); liver area is outlined in blue within Panel H. (For interpretation of the references to color in this figure legend, the reader is referred to the Web version of this article.)

maternal and cord blood (Yang et al., 2016) as well as amniotic fluid (Stein et al., 2012). Following a phase out of certain PFASs during the early 2000s, the overall use of this group of chemicals has declined over the past decade. However, serum levels of PFASs remain elevated (Hurley et al., 2018) and, as such, may be a health concern within the human population, particularly during prenatal development. Our study has revealed that PFOSA exposure leads to delayed development within early zebrafish embryos in a concentration- and exposure duration-dependent manner. In particular, for exposures initiated at 0.75 hpf, PFOSA induced delays in epiboly, a key stage during gastrulation when cell fate is determined. Epibolic movements within zebrafish are regulated by a combination of maternal/zygotic factors, developmental signaling pathways, and cytoskeletal reorganization, all of which precede and initiate germ layer formation, differentiation, and downstream developmental processes (Lepage and Bruce, 2010). Since these early stages of development are conserved across most species, including mammalian embryos prior to implantation (Niakan et al., 2012; Tadros and Lipshitz, 2009), PFOSA exposures during these stages may, at a sufficient concentration and exposure duration, result in disrupted gastrulation and implantation within the uterine wall.

Interestingly, PFOSA-induced impacts on mortality and development were not restricted to pre-epibolic stages and were independent of exposure initiation within the first 24 h of development, although longer exposure times did result in lower effect concentrations. Indeed, we did not identify a critical window for PFOSA-induced toxicity, suggesting that the mechanisms of delay were not restricted to targeted impacts on a key biological event or landmark during early development. However, our data suggest that PFOSA induced a delay in cell division, as initiation of PFOSA exposure at 0.75 hpf resulted in increased blastomeric cell sizes at 5 hpf and, during normal development, embryonic cell division leads to a progressive reduction of cell size during gastrulation (Langley et al., 2014). In addition, these data also suggest that PFOSA-induced impacts on cell size (and cell division) did not occur until after 3 hpf, possibly due to a lack of sufficient PFOSA uptake between 0.75 and 3 hpf. Interestingly, our recovery experiments showed that transient exposures during the first 6 h of development did not lead to significant developmental defects at 24 hpf, suggesting that 1) uptake of PFOSA during the first 6 h of development was not sufficient enough to induce morphological effects at 24 hpf and/or 2) depuration of PFOSA was rapid between 6 and 24 hpf, leading to a lack of detectable morphological effects at 24

hpf. A previous study with adult *Cyprinus carpio* showed that PFOSA has a half-life of ~7 d within adult fish (Chen et al., 2015), suggesting that depuration of PFOSA is relatively slow within adult teleosts. Therefore, although the species and life-stage within our study were different, the lack of effects at 24 hpf were likely due to insufficient uptake by 6 hpf.

We used mRNA-sequencing to reveal transcriptome-wide impacts associated with PFOSA-induced developmental delays. Although we observed developmental delays as early as 6 hpf, we conducted mRNA-sequencing based on RNA derived from 14- and 24-hpf embryos to minimize potential interference of maternally-loaded transcripts during early development. In addition, to preclude potential artifacts associated with PFOSA-induced developmental delays, we compared phenotype-matched, PFOSA-treated embryos (treated from 0.75 to 14 hpf or 0.75–24 hpf) to DMSO-treated embryos at 14 hpf. Interestingly, despite being phenotypically similar, the transcriptome of PFOSA-exposed embryos at 14 and 24 hpf was significantly affected compared to DMSO-exposed embryos at 14 hpf. Transcripts associated with hepatotoxicity-related pathways were the most significantly affected at 14 and 24 hpf, suggesting that, similar to a number of PFAS acids and their derivatives that are known to target the liver by dysregulation of lipid homeostasis (Das et al., 2017), PFOSA may primarily target liver morphology and/or function later in embryonic development. Indeed, DAVID- and IPA-based analyses also revealed a disruption of cholesterol synthesis/lipid metabolism as well as LXR/RXR-mediated pathways, both of which are associated with lipid homeostasis and liver development (Pinto et al., 2016).

Overall, our mRNA-sequencing data suggested that developmental exposures of PFOSA to zebrafish may lead to impacts on liver development and may be mediated through impacts on lipid transport and homeostasis. During zebrafish development, although the liver is not fully functional until ~72 hpf, the process of hepatic budding commences at approximately 24 hpf and transcripts regulating liver development are expressed as early as 6 hpf (Chu and Sadler, 2009; Villeneuve et al., 2014). Therefore, we exposed embryos to PFOSA from 0.75 to 24 hpf and assessed impacts on liver morphology and neutral lipid content at 128 hpf. Interestingly, exposure to 1.56–6.25 μ M PFOSA – concentrations that do not induce toxicity from 0.75 to 24 hpf – resulted in significant embryonic mortality and developmental defects at 128 hpf despite being reared in clean, PFOSA-free water from 24 to 128 hpf. In contrast to our results derived from exposures within an early window of development (0.75–6 hpf), these data suggest that PFOSA-induced effects at lower nominal concentrations occurred after termination of exposure at 24 hpf, possibly due to, similar to adult *Cyprinus carpio* (Chen et al., 2015), a longer half-life, longer depuration period and, as a result, biological persistence to 128 hpf. Indeed, surviving embryos at 1.56 μ M showed extensive pericardial and yolk sac edema. Therefore, we used a sublethal concentration of PFOSA (0.78 μ M) that did not result in gross morphological effects or developmental delays, as evidenced by lack of impacts on body length or yolk sac. However, even at this lower concentration, liver area was significantly decreased within PFOSA-exposed 128-hpf embryos following a 0.75 to 24 hpf exposure, suggesting that PFOSA either stunted liver development or induced liver atrophy.

Liver-specific effects were also associated with a small, albeit significant increase in neutral lipid content within the yolk sac. Since neutral lipid content within the yolk progressively reduces during yolk utilization due to lipid transport (Fraher et al., 2016), our data suggest that there may have been an inhibition of lipid transport from the yolk sac, an impact that may have led to indirect effects on the adjacent liver. Previous studies have shown that exposure to other PFASs – including GenX (a replacement for PFOA) and PFOS (a metabolic product of PFOSA) – induce morphologic

and transcriptomic impacts on the liver within *in vivo* and *in vitro* models (Conley et al., 2019; Zeng et al., 2019). Studies assessing PFAS levels within humans have shown that levels of PFOSA found in human serum, including blood of pregnant mothers, are of the order of ~10 ng/ml (~0.02 μ M) (Hurley et al., 2018; Poothong et al., 2017; Vestergaard et al., 2012). Although these values are more than an order of magnitude lower than concentrations used within this study, chronic exposure to PFOSA may have the potential to lead to bioaccumulation and impacts on liver development within developing human embryos.

5. Conclusion

In summary, our data collectively suggest that PFOSA exposure leads to developmental effects on zebrafish embryogenesis, with a developmental delay during early exposure windows, followed by impacts on the liver later in embryonic development. Importantly, PFOSA-induced impacts on liver development were observed at lower nominal concentrations despite being reared within clean water for 4 d following a ~24-h exposure. PFOSA-induced impacts on liver development were also associated with increased retention of neutral lipids within the yolk sac, suggesting that a lack of lipid transport may be driving PFOSA-induced effects on the developing liver. Therefore, future studies are needed to 1) better address the association between hepatotoxicity and lipid transport; 2) assess the uptake and depuration kinetics of PFOSA within developing zebrafish; and 3) focus on specific lipid metabolism- and transport-related transcripts and metabolites that may be involved in the developmental effects of PFOSA.

Funding

This work was supported by a National Science Foundation grant [1709719] to J.L. as well as a National Institutes of Health grant [R01ES027576] and USDA National Institute of Food and Agriculture Hatch Project [1009609] to D.C.V.

Acknowledgements

We thank Vanessa Cheng for occasional assistance with collection of zebrafish embryos as well as Drs. Daniel Schlenk and Justin Greer for assistance with pathway analysis.

Appendix A. Supplementary data

Supplementary data to this article can be found online at <https://doi.org/10.1016/j.envpol.2019.113550>.

References

- Annunziato, K.M., Jantzen, C.E., Gronske, M.C., Cooper, K.R., 2019. Subtle morphometric, behavioral and gene expression effects in larval zebrafish exposed to PFHxA, PFHxS and 6:2 FTOH. *Aquat. Toxicol.* 208, 126–137.
- Calafat, A.M., Kuklenyik, Z., Caudill, S.P., Reidy, J.A., Needham, L.L., 2006. Perfluorochemicals in pooled serum samples from United States residents in 2001 and 2002. *Environ. Sci. Technol.* 40 (7), 2128–2134.
- Chen, J., Tanguay, R.L., Tal, T.L., Gai, Z., Ma, X., Bai, C., Tilton, S.C., Jin, D., Yang, D., Huang, C., et al., 2014. Early life perfluorooctanesulphonate (PFOS) exposure impairs zebrafish organogenesis. *Aquat. Toxicol.* 150, 124–132.
- Chen, M., Qiang, L., Pan, X., Fang, S., Han, Y., Zhu, L., 2015. *In vivo* and *in vitro* isomer-specific biotransformation of perfluorooctane sulfonamide in common carp (*Cyprinus carpio*). *Environ. Sci. Technol.* 49 (23), 13817–13824.
- Chu, J., Sadler, K.C., 2009. New school in liver development: lessons from zebrafish. *Hepatology* 50 (5), 1656–1663.
- Conley, J.M., Lambright, C.S., Evans, N., Strynar, M.J., McCord, J., McIntyre, B.S., Travlos, G.S., Cardon, M.C., Medlock-Kakaley, E., Hartig, P.C., et al., 2019. Adverse maternal, fetal, and postnatal effects of hexafluoropropylene oxide dimer acid (GenX) from oral gestational exposure in sprague-dawley rats. *Environ. Health Perspect.* 127 (3), 37008.

Das, K.P., Wood, C.R., Lin, M.T., Starkov, A.A., Lau, C., Wallace, K.B., Corton, J.C., Abbott, B.D., 2017. Perfluoroalkyl acids-induced liver steatosis: effects on genes controlling lipid homeostasis. *Toxicology* 378, 37–52.

Dasgupta, S., Vliet, S.M.F., Cheng, V., Mitchell, C.A., Kirkwood, J., Vollaro, A., Hur, M., Mehdizadeh, C., Volz, D.C., 2019. Complex interplay among nuclear receptor ligands, cytosine methylation, and the metabolome in driving tris(1,3-dichloro-2-propyl) phosphate-induced epiboly defects in zebrafish. *Environ. Sci. Technol.* <https://doi.org/10.1021/acs.est.9b04127>.

Fair, P.A., Wolf, B., White, N.D., Arnett, S.A., Kannan, K., Karthikraj, R., Vena, J.E., 2019. Perfluoroalkyl substances (PFASs) in edible fish species from Charleston Harbor and tributaries, South Carolina, United States: exposure and risk assessment. *Environ. Res.* 171, 266–277.

Fei, C., McLaughlin, J.K., Tarone, R.E., Olsen, J., 2007. Perfluorinated chemicals and fetal growth: a study within the Danish National Birth Cohort. *Environ. Health Perspect.* 115 (11), 1677–1682.

Fraher, D., Sanigorski, A., Mellett, N.A., Meikle, P.J., Sinclair, A.J., Gibert, Y., 2016. Zebrafish embryonic lipidomic analysis reveals that the yolk cell is metabolically active in processing lipid. *Cell Rep.* 14 (6), 1317–1329.

Hu, X.C., Andrews, D.Q., Lindstrom, A.B., Bruton, T.A., Schaider, L.A., Grandjean, P., Lohmann, R., Carignan, C.C., Blum, A., Balan, S.A., et al., 2016. Detection of poly- and perfluoroalkyl substances (PFASs) in U.S. Drinking water linked to industrial sites, military fire training areas, and wastewater treatment plants. *Environ. Sci. Technol. Lett.* 3 (10), 344–350.

Hurley, S., Goldberg, D., Wang, M., Park, J.S., Petreas, M., Bernstein, L., Anton-Culver, H., Nelson, D.O., Reynolds, P., 2018. Time trends in per- and poly-fluoroalkyl substances (PFASs) in California women: declining serum levels, 2011–2015. *Environ. Sci. Technol.* 52 (1), 277–287.

Inoue, K., Okada, F., Ito, R., Kato, S., Sasaki, S., Nakajima, S., Uno, A., Saijo, Y., Sata, F., Yoshimura, Y., et al., 2004. Perfluorooctane sulfonate (PFOS) and related perfluorinated compounds in human maternal and cord blood samples: assessment of PFOS exposure in a susceptible population during pregnancy. *Environ. Health Perspect.* 112 (11), 1204–1207.

Kimmel, C.B., Ballard, W.W., Kimmel, S.R., Ullmann, B., Schilling, T.F., 1995. Stages of embryonic development of the zebrafish. *Dev. Dynam.* 203 (3), 253–310.

Kupsco, A., Dasgupta, S., Nguyen, C., Volz, D.C., 2017. Dynamic alterations in DNA methylation precede tris(1,3-dichloro-2-propyl)phosphate-induced delays in zebrafish epiboly. *Environ. Sci. Technol. Lett.* 4 (9), 367–373.

Langley, A.R., Smith, J.C., Stemple, D.L., Harvey, S.A., 2014. New insights into the maternal to zygotic transition. *Development* 141 (20), 3834–3841.

Lepage, S.E., Bruce, A.E., 2010. Zebrafish epiboly: mechanics and mechanisms. *Int. J. Dev. Biol.* 54 (8–9), 1213–1228.

Liu, H., Sheng, N., Zhang, W., Dai, J., 2015. Toxic effects of perfluorononanoic acid on the development of Zebrafish (*Danio rerio*) embryos. *J. Environ. Sci. (China)* 32, 26–34.

Mitchell, C.A., Dasgupta, S., Zhang, S., Stapleton, H.M., Volz, D.C., 2018. Disruption of nuclear receptor signaling alters triphenyl phosphate-induced cardiotoxicity in zebrafish embryos. *Toxicol. Sci.* 163, 307–318.

Monroy, R., Morrison, K., Teo, K., Atkinson, S., Kubwabo, C., Stewart, B., Foster, W.G., 2008. Serum levels of perfluoroalkyl compounds in human maternal and umbilical cord blood samples. *Environ. Res.* 108 (1), 56–62.

Niakan, K.K., Han, J., Pedersen, R.A., Simon, C., Pera, R.A.R., 2012. Human pre-implantation embryo development. *Development* 139 (5), 829–841.

Olsen, G.W., Huang, H.Y., Helzlsouer, K.J., Hansen, K.J., Butenhoff, J.L., Mandel, J.H., 2005. Historical comparison of perfluorooctanesulfonate, perfluorooctanoate, and other fluorochemicals in human blood. *Environ. Health Perspect.* 113 (5), 539–545.

Perez, F., Llorca, M., Kock-Schulmeyer, M., Skrbic, B., Oliveira, L.S., da Boit Martinello, K., Al-Dhabi, N.A., Antic, I., Farre, M., Barcelo, D., 2014. Assessment of perfluoroalkyl substances in food items at global scale. *Environ. Res.* 135, 181–189.

Pinto, C.L., Kalasekar, S.M., McCollum, C.W., Riu, A., Jonsson, P., Lopez, J., Swindell, E.C., Bouhlatouf, A., Balaguer, P., Bondesson, M., et al., 2016. Lxr regulates lipid metabolic and visual perception pathways during zebrafish development. *Mol. Cell. Endocrinol.* 419, 29–43.

Poothong, S., Thomsen, C., Padilla-Sanchez, J.A., Papadopoulou, E., Haug, L.S., 2017. Distribution of novel and well-known poly- and perfluoroalkyl substances (PFASs) in human serum, plasma, and whole blood. *Environ. Sci. Technol.* 51 (22), 13388–13396.

Reddam, A., Mitchell, C.A., Dasgupta, S., Kirkwood, J.S., Vollaro, A., Hur, M., Volz, D.C., 2019. mRNA-sequencing identifies liver as a potential target organ for triphenyl phosphate in embryonic zebrafish. *Toxicol. Sci.* <https://doi.org/10.1093/toxsci/kfz169>.

Sant, K.E., Jacobs, H.M., Borofski, K.A., Moss, J.B., Timme-Laragy, A.R., 2017. Embryonic exposures to perfluorooctanesulfonic acid (PFOS) disrupt pancreatic organogenesis in the zebrafish, *Danio rerio*. *Environ. Pollut.* 220 (Pt B), 807–817.

Sant, K.E., Sinno, P.P., Jacobs, H.M., Timme-Laragy, A.R., 2018. Nrf2a modulates the embryonic antioxidant response to perfluorooctanesulfonic acid (PFOS) in the zebrafish, *Danio rerio*. *Aquat. Toxicol.* 198, 92–102.

Sant, K.E., Venezia, O.L., Sinno, P.P., Timme-Laragy, A.R., 2019. Perfluorobutanesulfonic acid disrupts pancreatic organogenesis and regulation of lipid metabolism in the zebrafish, *Danio rerio*. *Toxicol. Sci.* 167 (1), 258–268.

Stahl, T., Mattern, D., Hubertus, B., 2011. Toxicology of perfluorinated compounds. *Environ. Sci. Eur.* 23 (1), 1–52.

Starkov, A.A., Wallace, K.B., 2002. Structural determinants of fluorochemical-induced mitochondrial dysfunction. *Toxicol. Sci.* 66 (2), 244–252.

Stein, C.R., Wolff, M.S., Calafat, A.M., Kato, K., Engel, S.M., 2012. Comparison of polyfluoroalkyl compound concentrations in maternal serum and amniotic fluid: a pilot study. *Reprod. Toxicol.* 34 (3), 312–316.

Tadros, W., Lipshitz, H.D., 2009. The maternal-to-zygotic transition: a play in two acts. *Development* 136 (18), 3033–3042.

Tittlemier, S.A., Pepper, K., Edwards, L., 2006. Concentrations of perfluorooctanesulfonamides in Canadian total diet study composite food samples collected between 1992 and 2004. *J. Agric. Food Chem.* 54 (21), 8385–8389.

Vestergaard, S., Nielsen, F., Andersson, A.M., Hjollund, N.H., Grandjean, P., Andersen, H.R., Jensen, T.K., 2012. Association between perfluorinated compounds and time to pregnancy in a prospective cohort of Danish couples attempting to conceive. *Hum. Reprod.* 27 (3), 873–880.

Villeneuve, D., Volz, D.C., Embry, M.R., Ankley, G.T., Belanger, S.E., Léonard, M., Schirmer, K., Tanguay, R., Truong, L., Wehrmas, L., 2014. Investigating Alternatives to the fish early-life stage test: a strategy for discovering and annotating adverse outcome pathways for early fish development. *Environ. Toxicol. Chem.* 33 (1), 158–169.

Vliet, S.M., Dasgupta, S., Volz, D.C., 2018. Niclosamide induces epiboly delay during early zebrafish embryogenesis. *Toxicol. Sci.* 166 (2), 306–317.

Vliet, S.M., Ho, T.C., Volz, D.C., 2017. Behavioral screening of the LOPAC1280 library in zebrafish embryos. *Toxicol. Appl. Pharmacol.* 329, 241–248.

Vliet, S.M., Dasgupta, S., Sparks, N.R.L., Kirkwood, J.S., Vollaro, A., Hur, M., Zur Nieden, N.I., Volz, D.C., 2019. Maternal-to-zygotic transition as a potential target for niclosamide during early embryogenesis. *Toxicol. Appl. Pharmacol.* 114699. <https://doi.org/10.1016/j.taap.2019.114699>.

Whitworth, K.W., Haug, L.S., Sabaredzovic, A., Egglesbo, M., Longnecker, M.P., 2016. Brief report: plasma concentrations of perfluorooctane sulfonamide and time-to-pregnancy among primiparous women. *Epidemiology* 27 (5), 712–715.

Yang, L., Wang, Z., Shi, Y., Li, J., Wang, Y., Zhao, Y., Wu, Y., Cai, Z., 2016. Human placental transfer of perfluoroalkyl acid precursors: levels and profiles in paired maternal and cord serum. *Chemosphere* 144, 1631–1638.

Zeng, Z., Song, B., Xiao, R., Zeng, G., Gong, J., Chen, M., Xu, P., Zhang, P., Shen, M., Yi, H., 2019. Assessing the human health risks of perfluorooctane sulfonate by in vivo and in vitro studies. *Environ. Int.* 126, 598–610.